Article

Telomerase and Pluripotency Factors Jointly Regulate Stemness in Pancreatic Cancer Stem Cells

Karolin Walter [1], Eva Rodriguez-Aznar [1], Monica S. Ventura Ferreira [2], Pierre-Olivier Frappart [1,3], Tabea Dittrich [1], Kanishka Tiwary [1], Sabine Meessen [4], Laura Lerma [5], Nora Daiss [1], Lucas-Alexander Schulte [1], Zeynab Najafova [6], Frank Arnold [1], Valentyn Usachov [1], Ninel Azoitei [1], Mert Erkan [7,8], Andre Lechel [1], Tim H. Brümmendorf [2], Thomas Seufferlein [1], Alexander Kleger [1], Enrique Tabarés [5], Cagatay Günes [4], Steven A. Johnsen [9], Fabian Beier [2], Bruno Sainz, Jr. [10,11,12] and Patrick C. Hermann [1,*]

1   Department of Internal Medicine I, University Medical Centre Ulm, 89081 Ulm, Germany; karolin.walter@uni-ulm.de (K.W.); eva.rodriguez-aznar@uni-ulm.de (E.R.-A.); pfrappar@uni-mainz.de (P.-O.F.); tabea.dittrich@uni-ulm.de (T.D.); kanishka.tiwary@uni-ulm.de (K.T.); nora.daiss@uniklinik-ulm.de (N.D.); lucas-alexander.schulte@uniklinik-ulm.de (L.-A.S.); frank.arnold@uni-ulm.de (F.A.); usachovtn@yahoo.com (V.U.); ninel.azoitei@uniklinik-ulm.de (N.A.); andre.lechel@uniklinik-ulm.de (A.L.); thomas.seufferlein@uni-ulm.de (T.S.); alexander.kleger@uni-ulm.de (A.K.)
2   Department of Hematology, Oncology, Hemostaseology and Stem Cell Transplantation, University Hospital of the RWTH Aachen, 52062 Aachen, Germany; monicasvferreira@gmail.com (M.S.V.F.); tbruemmendorf@ukaachen.de (T.H.B.); fbeier@ukaachen.de (F.B.)
3   Institute of Toxicology, University Medical Centre of the Johannes Gutenberg University Mainz, 55131 Mainz, Germany
4   Department of Urology, Ulm University, 89081 Ulm, Germany; sabine.meessen@uni-ulm.de (S.M.); cagatay.guenes@uniklinik-ulm.de (C.G.)
5   Department of Preventive Medicine, Public Health and Microbiology, Universidad Autónoma de Madrid (UAM), 28049 Madrid, Spain; lerma.laura@gmail.com (L.L.); enrique.tabares@uam.es (E.T.)
6   Department of Surgery, University Medical Center Göttingen, 37075 Göttingen, Germany; zeynab.najafova@med.uni-goettingen.de
7   Department of Surgery, Koç University School of Medicine, Istanbul 34450, Turkey; merkan@ku.edu.tr
8   Research Center for Translational Medicine, Koç University, Istanbul 34450, Turkey
9   Gene Regulatory Mechanisms and Molecular Epigenetics Lab, Gastroenterology Research, Mayo Clinic, Rochester, MN 55905, USA; Johnsen.Steven@mayo.edu
10 Department of Biochemistry, Universidad Autónoma de Madrid (UAM), 28049 Madrid, Spain; bsainz@iib.uam.es
11 Department of Cancer Biology, Instituto de Investigaciones Biomédicas "Alberto Sols" (IIBM), CSIC-UAM, 28049 Madrid, Spain
12 Chronic Diseases and Cancer, Area 3—Instituto Ramón y Cajal de Investigación Sanitaria (IRYCIS), 28049 Madrid, Spain
*   Correspondence: patrick.hermann@uni-ulm.de; Tel.: +49-731-500-44736

Simple Summary: Pancreatic ductal adenocarcinoma (PDAC) is an extremely lethal cancer with very limited therapeutic options. Cancer stem cells (CSCs) are essential for propagation of PDAC, but also for its metastatic activity and chemoresistance. To date, it is still unclear how cancer stem cells (CSCs) regulate their 'stemness' and self-renewal properties, and to what extent they share common features with normal stem cells. Telomerase regulation is a key factor in stem cell maintenance. Here, we investigate how telomerase regulation affects CSC biology in PDAC, and delineate the mechanisms by which telomerase activity and CSC properties are linked.

Abstract: To assess the role of telomerase activity and telomere length in pancreatic CSCs we used different CSC enrichment methods (CD133, ALDH, sphere formation) in primary patient-derived pancreatic cancer cells. We show that CSCs have higher telomerase activity and longer telomeres than bulk tumor cells. Inhibition of telomerase activity, using genetic knockdown or pharmacological inhibitor (BIBR1532), resulted in CSC marker depletion, abrogation of sphere formation in vitro and reduced tumorigenicity in vivo. Furthermore, we identify a positive feedback loop between stemness factors (NANOG, OCT3/4, SOX2, KLF4) and telomerase, which is essential for the self-renewal of CSCs. Disruption of the balance between telomerase activity and stemness factors eliminates

CSCs via induction of DNA damage and apoptosis in primary patient-derived pancreatic cancer samples, opening future perspectives to avoid CSC-driven tumor relapse. In the present study, we demonstrate that telomerase regulation is critical for the "stemness" maintenance in pancreatic CSCs and examine the effects of telomerase inhibition as a potential treatment option of pancreatic cancer. This may significantly promote our understanding of PDAC tumor biology and may result in improved treatment for pancreatic cancer patients.

Keywords: cancer stem cells; telomerase; telomere length; self-renewal; stemness; pancreatic cancer

1. Introduction

Pancreatic ductal adenocarcinoma (PDAC) is the most frequent and the most lethal form of pancreatic cancer, and it is expected to be the second most frequent cause of cancer-related death by 2030 [1]. Diagnosis of PDAC is frequently delayed due to the absence of early symptoms, pronounced resistance to therapy and early metastatic spread. As a consequence, less than 20% of patients diagnosed with PDAC are eligible for resection [2], the only curative treatment option. Despite growing knowledge about PDAC tumor biology, advances in treatment are still scarce, with FOLFIRINOX and gemcitabine + nab-paclitaxel currently representing the most promising combination chemotherapies [3,4]. The complexity and heterogeneity of pancreatic cancer remains only partially deciphered, and strategies for developing novel and more effective treatments are urgently needed.

Cancer stem cells (CSCs) have been implicated in a wide variety of tumors. We and others have previously demonstrated their outstanding importance in pancreatic cancer perpetuation, metastasis, and therapy resistance [5,6]. While self-renewal is a defining characteristic of CSCs [7], the precise mechanism how CSCs maintain their stemness state remains unclear. Therefore, understanding CSCs at the molecular level might reveal targetable principles that could potentially be exploited therapeutically. As telomerase activity and telomere regulation have been proposed to play an essential role in tumor cell maintenance and are considered "hallmarks of cancer" by Hanahan and Weinberg, telomerase activity might present such a potential target.

Vertebrate telomeres consist of repetitive TTAGGG DNA sequences. The telomerase complex consists of a catalytic subunit (telomerase reverse transcriptase, TERT) and a telomerase RNA component (TERC). TERC serves as a template for the addition of DNA tandem repeats catalyzed by TERT, which is the rate-limiting factor for telomerase activity [8]. Further factors such as the shelterin proteins TERF1 and TERF2 represent important factors for telomerase regulation [9]. Telomeres protect the ends of the chromosomes from end-to-end fusion and exonucleolytic degradation, preventing genome instability. Importantly, in most human cells telomeric DNA is shortened with each cell division, leading to undetectable telomerase activity in the vast majority of somatic tissues [10] and accumulation of critically short telomeres, subsequently limiting cellular replicative capacity and ultimately resulting in replicative senescence [11].

Telomere length stabilization by the reactivation of telomerase or (much less frequently) through alternative mechanisms of telomere lengthening (ALT) results in elevated telomerase activity in 85–90% of human tumors, highlighting this as the prime mechanism to maintain telomere functionality in cancer [12].

Several studies have examined the effects of telomerase inhibition on tumor growth. In cancer cell lines, the potent non-nucleosidic telomerase inhibitor BIBR1532 induces telomere shortening, proliferation arrest and senescence [13]. Currently the effects of the clinical grade telomerase inhibitor GRN163L (Imetelstat) are being tested in several tumors, such as breast, lung cancer and myeloma. However, the effects of telomerase inhibition on CSCs have yet to be elucidated.

In the present study we investigate the role of telomere regulation and telomerase inhibition in the maintenance of pancreatic CSCs. We demonstrate that CSCs isolated

from patient-derived xenografts (PDXs) present higher telomerase activity, resulting in significantly longer telomeres compared to bulk tumor cells. Intriguingly, the lengthening of telomeres is inextricably linked to increased expression of the pluripotency/stemness factors OCT3/4, SOX2, NANOG and KLF4, and is jointly regulated in a previously undescribed positive feedback loop, which is necessary for these cells to escape senescence, and regulates their stemness properties. Furthermore, pharmacological inhibition of telomerase using BIBR1532 as well as genetic knock-down of TERT greatly decreased the CSC frequency of patient-derived PDAC cells in vitro and in vivo by CSC-specific induction of DNA damage and apoptosis.

2. Materials and Methods

2.1. Mice, Transplantation and Treatment

Female 6–8 week-old athymic Nude-Foxn1nu mice were purchased from Envigo (Gannat, France). For subcutaneous xenografting, single cells were resuspended in 40 µL 1:1 media:Matrigel (Invitrogen, Schwerte, Germany). CSC frequencies and statistical significance of the comparison were determined from extreme limiting dilution assay results using ELDA software [14]. For in vivo treatment, animals received biweekly intraperitoneal (i.p.) injections of doxycycline (1 mg/mL). Tumor size was calculated using the formula (length $\times$ width^2)/2. All animal experiments were conducted under the ethical and animal protection regulations of the German and Spanish Animal Protection Law and were previously approved by the governmental review board of the state of Baden-Württemberg (V-1347). This included the housing of the animals in specific pathogen-free conditions.

2.2. Primary Pancreatic Cancer Cells and Other Cell Lines

Primary human pancreatic cancer cell lines were generated from established PDX obtained under MTAs (Reference no. I409181220BSMH and I405271505PHMH) from the CNIO, Madrid, Spain, and maintained in culture as described previously [15]. U-2OS and HPDE cells have been previously described [16]. Hek293T cells were cultured in Dulbecco's modified Eagle's medium (DMEM) supplemented with 10% fetal bovine serum (FBS), 1% penicillin/ streptomycin and 1% glutamine, in standard conditions (37 °C, 5% CO$_2$). BIBR1532 (Selleckchem, Houston, TX, USA) was used at 80 µM (3 or 7 days treatment, changing media and BIBR1532 every other day), Gemcitabine (Merck, Darmstadt, Germany) was used at 5 µM and Olaparib (Selleckchem) was used at 25 µM (for 72 h) for 3D cell culture unless stated otherwise.

2.3. CSC Enrichment

2.3.1. CD133 and ALDH Fluorescence Activated Cell Sorting (FACS)

For CSC enrichment primary pancreatic cancer cells were stained with CD133 (See Supplementary Table S1) or the ALDEFLUOR™ Kit (STEMCELL™ Technologies, Vancouver, BC, Canada) was performed. Cell sorting was performed using a FACSAria III (BD Bioscience, Franklin Lakes, NJ, USA).

2.3.2. Sphere Culture

Spheres were cultured as described previously [5]. Briefly, cells were cultured in DMEM-F12 supplemented with B-27 (ThermoFisher Scientific, Waltham, MA, USA) and bFGF (Novoprotein, Summit, NJ, USA). 10,000 cells per milliliter were seeded in ultra-low attachment plates (Corning, New York, NY, USA). Spheres were defined as 3-dimensional multicellular structures of $\geq$40 µm. After 7 days, sphere formation was quantified either manually using a Leica stereomicroscope or using a CASY TT (OLS OMNI Life Science, Bremen, Germany) with a 150 µm capillary. Dead cells and debris were excluded from the quantification.

2.4. Pseudorabies Virus Infections

The virulent pseudorabies virus (PRV) strain PRV-NIA3 has been previously described. The parental PRV virus vBecker2 was generated by transfection of pBecker2 plasmid into

Hela Tet-Off cells. PRV-TER, a recombinant PRV virus in which the endogenous viral IE180 promoter was substituted with the TERT human tumor promoter, has been detailed previously [16]. For infection of HPDE and Panc185 cells in adherence, 5×10^5 cells were seeded in 6 multi-well plates. Twenty-four hours post seeding, cells were infected with PRV-NIA3, vBecker2 or PRV-TER at a multiplicity of infection (MOI) of 0.1 TCID50/cell. After an absorption period of 2 h at 37 °C, the cells were washed with PBS to remove unabsorbed virus and then incubated for 72 h at 37 °C. Virus yield was determined from total lysates of infected cells on U2OS cells as previously described [16]. For infection of spheres, 7-day-old Panc185 1st generation spheres were trypsinized, cells were counted, and cell suspensions of 5×10^5 cells were seeded in 6 multi-well plates and infected with PRV-NIA3, vBecker2 or PRV-TER at a multiplicity of infection (MOI) of 0.1 TCID50/cell. After an absorption period of 2 h at 37 °C under agitation, cultures were washed with PBS to remove unabsorbed virus, and incubated for 72 h at 37 °C. Virus yield was determined as detailed above.

2.5. Telomerase Activity

For telomerase activity measurement, the TeloTAGGG telomerase PCR ElisaPLUS kit (Roche, Mannheim, Germany), the telomeric repeat amplification protocol (TRAP) or qRT-PCR based TRAP were performed. Primer sequences are provided in the Supplementary Information (See Supplementary Table S2).

2.6. Organoid Culture

Tumor pieces of patient-derived xenografts (PDXs) were digested with Accutase® solution (Merck) for 30 min at 37 °C. The cells were then filtered in EASY strainer 100 μM (greiner bio-one, Frickenhausen, Germany) and cultured in Matrigel coated plates containing organoid culture medium as described in Frappart et al. 2020 with 5% growth factor reduced Matrigel (Corning). Media of the organoid culture plates was refreshed every 3–4 days. Organoids were treated with BIBR1532 and gemcitabine at 12.5, 25.0 and 50 μM for 72 h. To determine the number of metabolically active and viable organoids, the CellTiter-Glo® 3D Cell Viability Assay (Promega, Madison, WI, USA) was performed following the manufacturer's instructions.

2.7. Plasmids, Infection and Transfection

For RNAi-mediated gene silencing, the pGIPZ and pTRIPZ lentiviral vectors developed by Dr. Greg Hannon (Cold Spring Harbor Laboratory, New York, NY, USA) and Dr. Steve Elledge (Harvard Medical School, Boston, MA, USA) and the corresponding shRNA constructs (GIPZ TERT shRNAs, RHS4531-EG7015 and TRIPZ TERT shRNAs, RHS4740-EG7015) were purchased from Dharmacon (Lafayette, CO, USA). The NANOG reporter lentiviral vector backbone and the sequence of the construct have been previously described [17]. NANOG, OCT3/4, SOX2 and KLF4 were cloned into the PB-EF1-MCS-IRES-RFP plasmid (SBI, Palo Alto, CA, USA). Transposition was performed using Super PiggyBac transposase (SBI), transfection was performed with standard Lipofectamine® 2000 (Invitrogen).

2.8. Flow Cytometry

Antibodies used in this study are listed in the Supplementary Table S1. For ALDH detection the ALDEFLUOR™ kit (STEMCELL™ Technologies) was used. Apoptosis was measured using Annexin V-APC (BD Bioscience) and CellEvent™ Caspase-3/7 green detection reagent (Invitrogen). For DNA content staining cells were stained with DAPI. Cellular senescence was measured using the SA-ß-gal kit (BioCat, Heidelberg, Germany). Samples were analyzed by flow cytometry using a LSR II (BD Bioscience), and data were analyzed with FlowJo V10 (Ashland, OR, USA). FACSorting was performed using a FACSAria III (BD Bioscience).

2.9. Q-FISH

Telomere Q-FISH was performed as previously described [18]. Fluorescence intensity of the telomeres was quantified with Definiens software (Definiens, Munich, Germany).

2.10. Immunofluorescence

Primary pancreatic cancer cells were FACSorted, seeded on cover-slips in 6-well dishes, incubated at 37 °C for 12 h, washed with PBS and fixed with 2% PFA for 20 min at room temperature. Coverslips were washed 3 times with PBS and incubated at room temperature for 15 min in 0.7% triton in PBS. 1 h blocking with 5% milk powder in 0.1% TBS-T at room temperature was followed by incubation with the respective antibodies (1:500) in a humidified chamber at 4 °C overnight. Coverslips were then washed 3× with 0.1% TBS-T. Secondary antibodies (1:1000) were incubated at room temperature in a humidified chamber for 2 h, washed and mounted with ProLongTMGold Antifade mounting reagent with DAPI (ThermoFisher Scientific). Images were captured using a Leica TCS SP8-HCS confocal microscope. Antibodies are listed in the Supplementary Table S1.

2.11. RNA Isolation and qRT-PCR

Total RNA was prepared using RNeasy kits with on-column genomic DNA digestion following the manufacturer's instructions (Qiagen, Hilden, Germany). First strand cDNA was prepared using QuantiTect Reverse Transcription kit (Qiagen). Reactions were performed with QuantiFastSybr Green PCR Kit (Qiagen) using a QuantStudio 3 machine (Applied Biosystems, Waltham, MA, USA). Results were analyzed using the 2-ddCt method and calculated as relative to HPRT expression. Reactions were carried out from at least three independent experiments. Primer sequences are provided in the Supplementary Table S2.

2.12. MTT Assay

1000 cells were seeded in a 96-well plate and incubated for 24 h at 37 °C. Cells were incubated for 72 h with the indicated concentrations of the respective drugs and further incubated for 3 h with 5 mg/mL MTT (Merck). Finally, DMSO (Roth, Karlsruhe, Germany) was added, and the optical density was measured at 560 nm using an Infinite Pro 200 plate reader (Tecan, Männedorf, Switzerland).

2.13. Statistical Analysis

Results for continuous variables are presented as means ± SEM. Unless stated otherwise, treatment groups were compared with the one-sided Mann–Whitney-U test, tumor growth dynamics were compared by calculating areas under the curve. Chi-squared tests were used to compare CSC frequencies. Contingency tables were compared using Fisher's exact test. *p*-Values <0.05 were considered statistically significant. Statistical analyses were performed using GraphPad Prism 5.0 (San Diego, CA, USA).

3. Results

3.1. Telomerase Activity and Telomere Length in Pancreatic CSCs vs. Bulk Tumor Cells

In a first screen we tested several primary PDAC cell lines for their average telomere length using flow-FISH (Supplementary Figure S1) and observed that all tested samples showed very short telomeres (<5th age percentile) (Figure 1A). In order to evaluate telomerase activity specifically in CSCs, we compared the expression levels of *TERT* and *TERF1* in CSCs versus bulk tumor cells in three human PDX-derived primary PDAC cell lines (Panc215, Panc185, Panc354). Using well-established CSC enrichment methods (i.e., CD133 or ALDEFLUOR fluorescence activated cell sorting (FACS), and sphere culture (Figure 1B)), we found increased expression of *TERT* and/or *TERF1* in CD133+ cells (Figure 1C), ALDE-FLUOR+ cells (Figure 1D) and in sphere cultures (Figure 1E) compared to the negative population or adherent cells, respectively. In immunofluorescence staining, significantly more TERT-expressing cells were detected in the CD133+ CSC subpopulation as compared to CD133− cells (Figure 1F). Next, we measured telomerase activity as the functionally relevant readout. Using gel-based as well as PCR-based TRAP (telomeric repeat amplification protocol) assays, significantly higher telomerase activity was detected in the CSC fraction as compared to the respective control cells (Figure 1G–I). As the key function of telomerase

is telomere elongation, we performed Q-FISH-analysis to determine telomere length in CD133+ (Figure 1J) or ALDH+ (Supplementary Figure S2) CSCs and in the respective marker-negative control populations (Panc215: CD133+ 66.2 a.u. vs. CD133− 31.7 a.u.; Panc185: CD133+ 40.8 a.u. vs. CD133− 31.5 a.u.; Panc354: CD133+ 41.6 a.u. vs. CD133− 35.4 a.u.; and Panc286: ALDH+ 11.2556 a.u. vs. ALDH− 9.1304 a.u.).
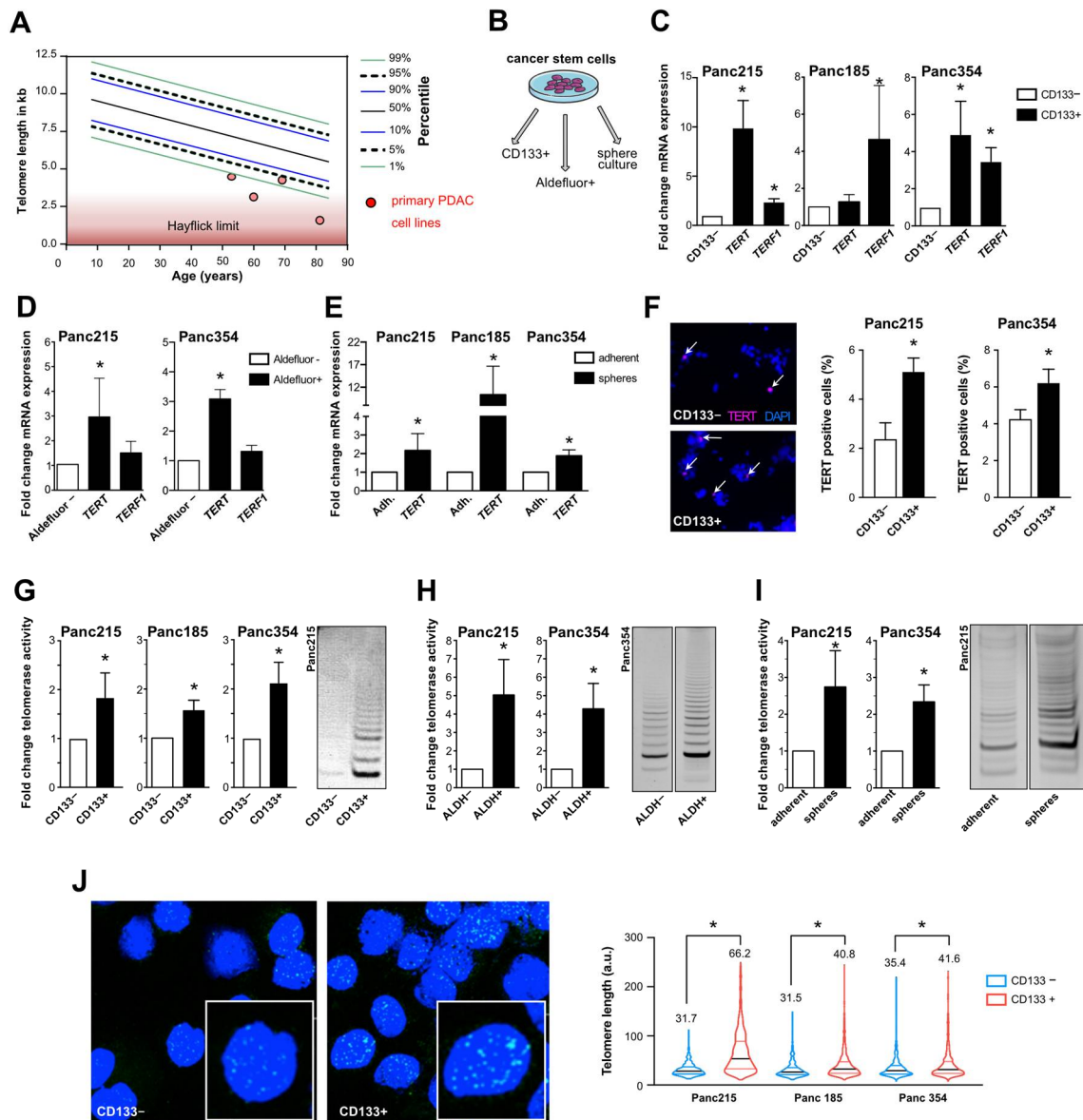

Figure 1. Telomerase activity stabilizes telomere length in pancreatic CSCs: (**A**) telomere length in primary PDAC cells (red dot) with respect to patient age measured by FlowFISH; (**B**) schematic illustration showing the CSC enrichment methods for CD133 and ALDEFLUOR via FACS or in sphere culture; (**C–E**) RT-qPCR analysis of *TERT* and *TERF1* mRNA levels in primary pancreatic cancer stem cells enriched and selected by FACS for CD133 (**C**), or ALDEFLUOR (**D**), and cultured as spheres (**E**) (CSCs) vs. corresponding control (non-CSCs) (*n* = at least 3 independent experiments). (**F**) Immunofluorescence staining and quantification for TERT (red) in CD133− and CD133+ FACSorted cells (*n* = 5 independent experiments). Cells were counterstained with DAPI (nuclear marker, blue), 4× magnification is shown. (**G–I**) Telomerase activity measurement in CD133 (**G**) or ALDEFLUOR (**H**) negative vs. positive cells and in adherent vs. sphere cell-cultures (**I**) (*n* = 3 independent FACSortings and sphere culture experiments). (**J**) Representative pictures of Q-FISH with telomeres (green) and DAPI (blue) and violin plot showing telomere length analysis in CD133 negative (non-CSCs) and positive cells (CSCs) 40× magnification is shown. The mean is depicted in numbers and as black line. *n* ≥ 3 from independent FACSortings with each >150 measurements per group. In (**C–J**), data are presented as mean ± SEM. * $p \leq 0.05$ (Mann–Whitney-U test).

In the CSC population we observed significantly longer telomeres compared to the non-CSCs. These results confirm increased telomerase expression and activity in pancreatic CSCs as compared to non-CSCs.

3.2. A Positive Feedback Loop between Stemness Factors and Telomerase Maintains CSC Phenotype

As we observed a significant increase in the regulation and activity of telomerase in CSCs, we investigated whether increased telomerase activity is associated with the expression of genes and markers of stemness and pluripotency. We observed increased expression of *OCT3/4, NANOG, SOX2* and *LGR5* in the CSC population (Figure 2A) as compared to the CD133− control population. Similarly, expression levels of these genes were significantly elevated in ALDEFLUOR-positive cells (Figure 2B) and spheres (Supplementary Figure S3) compared to the negative cells, demonstrating increased expression of most stemness-associated genes in CSCs. To overcome CSC marker-dependent variation, we next infected Panc354 primary cell cultures with a Nanog-YNL reporter system, which reports for Nanog activity using a Yellow Nano-Lantern [19]. YNL+ cells showed increased expression of *NANOG*, but also of *TERT* and other stemness-associated genes (Figure 2C). Furthermore, YNL+ cells showed significantly higher telomerase activity (Figure 2D). While the amount of CD133+ cells was unchanged (Figure 2E), sphere forming capacity was significantly increased (Figure 2F) in the YNL+ cells.

To confirm higher telomerase activity in CSCs, we used a recombinant pseudorabies virus (PRV) that we previously designed and demonstrated to replicate only in cells with high telomerase activity (PRV-TER) [16]. Adherent cultures of human pancreatic ductal epithelial (HPDE) cells and Panc185 cells were infected with two parental control viruses (PRV-NIA3 and vBecker2) and with PRV-TER. While both parental viruses efficiently replicated in HPDE and Panc185 cultures, PRV-TER was unable to produce de novo virions in either culture (Figure 2G). In contrast, when CSC-enriched sphere cultures were infected, all three viruses efficiently replicated and produced de novo virions, confirming that CSC-enriched sphere cultures express significantly higher telomerase activity, allowing for PRV-TER to efficiently replicate in these cultures. In order to determine the repopulation potential of BIBR-treated CSCs, we next performed clonogenic assays after withdrawal of BIBR treatment. Interestingly, while both YNL+ and YNL− cells re-grew after vehicle treatment, the treatment selectively inhibited YNL+ CSCs to re-grow in culture, while YNL− cells were hardly affected by BIBR and were able to repopulate the cell culture (Figure 2H).

Finally, we explored the mechanism(s) underlying increased telomerase regulation in CSCs. Direct promoter activation can lead to increased *TERT* activity in tumor cells, and two common promoter mutations (-124 and -146 bp upstream of the *TERT* start site) have been associated with increased telomerase activity [20]. These mutations are frequent in some cancers, but rarely occur in gastrointestinal cancers. The promoter sequencing of all tested PDAC cells revealed wildtype sequences (6/6 primary cell lines, 5/5 established cell lines, Supplementary Figure S4). We generated PiggyBac expression vector constructs that specifically express *SOX2, OCT3/4, KLF4* or *NANOG* to determine how these stemness factors modulate *TERT* expression. Supporting this approach, Hsieh et al. showed that PARP1 recruits KLF4 to activate telomerase expression in embryonic stem cells [21]. Interestingly, the expression of *OCT3/4* and *SOX2* significantly upregulated *TERT* expression and a similar trend was observed for *NANOG* and *KLF4* (Figure 2I). Furthermore, overexpression of any of these factors resulted in concomitant upregulation of the other factors and enhanced telomerase activity (Figure 2J), indicating an intricate cross-regulation of these individual stemness factors.

Taken together, these data show that telomerase activity is increased in CSCs and is regulated by a feedback loop between *TERT* and key pluripotency-associated factors.
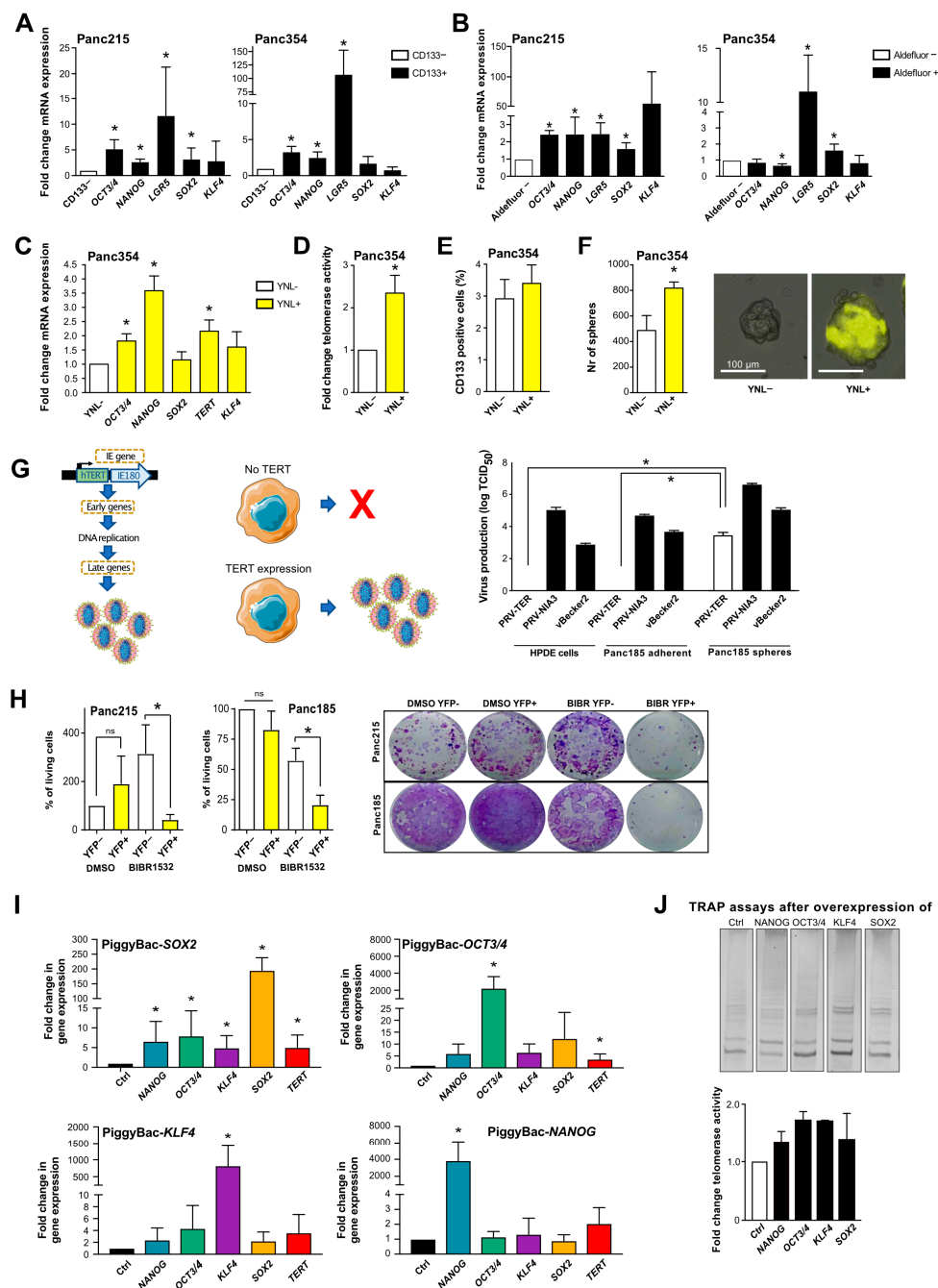
Figure 2. Interplay between pluripotency/stemness factors and telomerase activity in pancreatic CSCs: (**A**,**B**) RT-qPCR analysis of pluripotency/stemness-associated genes in primary pancreatic CSCs enriched by CD133 expression (**A**) or ALDE-FLUOR activity (**B**) vs. CD133− and ALDEFLUOR- non-CSCs (*n* = at least 3 independent FACSortings). (**C–F**) Quantitative RT-PCR (**C**), telomerase activity (**D**), flow cytometry analysis for CD133 (**E**) and sphere formation capability (**F**), compared in NANOG negative cells (white) vs. NANOG positive cells (yellow) using a NANOG-YNL reporter. (**G**) Schematic illustration and quantification on the production of virions in parental pseudorabies viruses (PRV-NIA3 and vBecker) compared to telomerase activity-dependent virus production (PRV-TER) in adherent HPDE and Panc185 cells as compared to Panc185 spheres. (**H**) Clonogenic Assay in NANOG-YNL positive and negative cells after withdrawing BIBR1532 (*n* = ≥3 independent experiments. ns = not statistically significant) (**I**) Gene expression levels of stemness/pluripotency genes and *TERT* in HEK293T cells after inducing expression of *SOX2, OCT3/4, KLF4* and *NANOG*, compared to the empty vector control (*n* = 4 independent experiments). In (**A–I**), data are represented as mean ± SEM. * *p* ≤ 0.05 (Mann–Whitney-U test). (**J**) Telomerase activity after inducing expression of *SOX2, OCT3/4, KLF4* and *NANOG*, compared to the empty vector control. Representative TRAP assays and quantification are depicted.

3.3. Telomerase Inhibition Causes DNA Damage and Apoptosis in CSCs

Based on the observed link between telomerase activity/telomere length and a CSC phenotype, we evaluated the effects of telomerase inhibition on the CSC population. For this purpose, we treated primary pancreatic cancer cells with the small molecule telomerase inhibitor BIBR1532 and selected 80 µM as an effective sub-IC50 concentration (Supplementary Figure S5). BIBR1523 treatment was performed for 3 d or 7 d, respectively, and after 7 d of treatment telomerase activity was effectively decreased (Figure 3A). Functionally, treatment with BIBR1523 significantly reduced telomere length (Figure 3B). Interestingly, the treatment effect was potentiated with longer treatment in the CD133+ CSC population. However, in the CD133− bulk tumor cell population telomere length increased again after 7 d of treatment. This is most likely due to early elimination of CD133− cells with critically short telomeres and the inability of CD133− cells to upregulated telomerase, leading to a relative enrichment in CD133− cells with longer telomeres. Based on these results, treatment with BIBR1523 was performed for 7d in all further experiments. To determine the biological consequence of telomerase inhibition, we quantified DNA damage by γ-H2AX staining, as telomerase inhibition can induce DNA damage, cell cycle arrest and apoptosis in other systems [22]. Treatment with BIBR1532 increased γ-H2AX foci generation much more strongly in CD133+ CSCs than in bulk tumor cells, indicating a preferential induction of DNA damage after telomerase inhibition in CSCs (Figure 3C). Accumulation of DNA double strand breaks (DSBs) and the activation of DNA damage response are considered contributing factors to cellular senescence [11]; Therefore, we next measured senescence using flow cytometry to detect ß-galactosidase after BIBR1532 treatment and observed increased senescence in both CD133− and CD133+ cells, excluding preferential induction of senescence in CSCs in response to BIBR1532 treatment (Figure 3D).

As DSBs can also induce apoptosis, we next measured early apoptotic cells by AnnexinV staining and observed significantly more apoptotic cells in the CD133+ CSC population upon BIBR1532 treatment, while CD133− cells were unaffected (Figure 3E). Furthermore, we performed Caspase 3/7 staining to determine whether BIBR1532-induced DNA damage leads to the recruitment of apoptosis effector kinases. In line with the AnnexinV staining, BIBR1532 treatment resulted in increased Caspase 3/7 staining in the CD133+ CSC population, while no differences were observed in CD133− cells (Figure 3F).

3.4. CSCs Are Depleted upon Telomerase Inhibition

As BIBR1532 treatment appeared to have CSC-specific effects, we next evaluated the effect of telomerase inhibition on CSC properties. As expected, BIBR1532 treatment strongly reduced the expression of TERT, along with established stemness/pluripotency-associated genes (Figure 4A), and significantly decreased the percentage of CSCs as measured by expression of CD133 or ALDEFLUOR (Figure 4B, Supplementary Figure S6A,B) or sphere formation capacity (Figure 4C).

Most importantly, BIBR1532 treatment strongly reduced the number of tumor-initiating cells in extreme limiting dilution (ELDA) tumorigenicity assays in nude mice as the gold standard readout for CSC potential. Furthermore, tumor growth after BIBR1532 treatment was significantly slower compared to vehicle-treated cells, and CSC content in growing tumors was reduced (Figure 4D and Supplementary Figure S6C). These data clearly indicate that telomerase inhibition by BIBR1532 strongly inhibits the functional capacity of the CSC population.
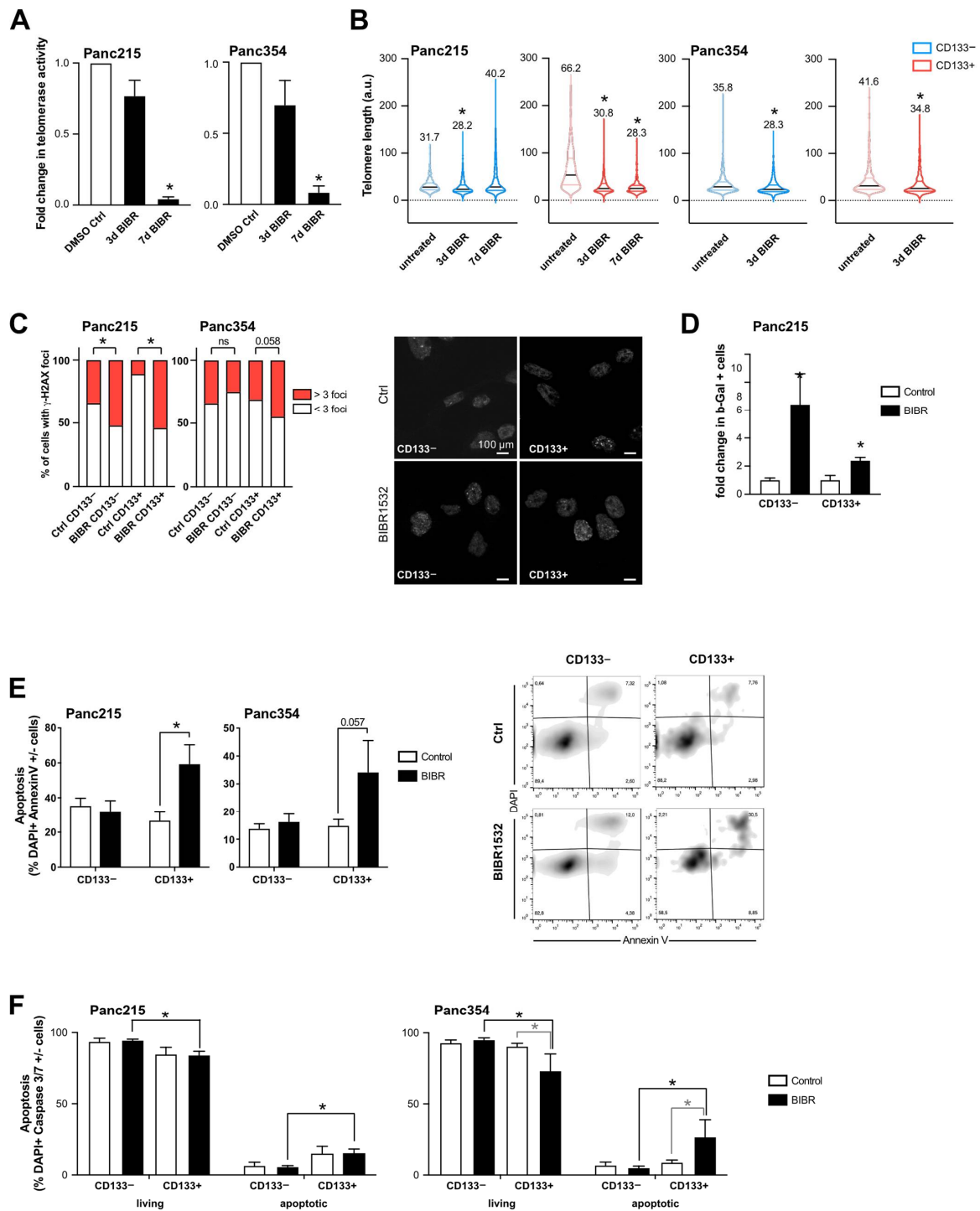
Figure 3. Targeting telomerase activity with a small molecule inhibitor (BIBR1532): (**A**,**B**) The effects of BIBR1532 treatment on telomerase activity (**A**), and telomere length (**B**) in CD133− cells (blue) and in the CD133+ CSC population (red) were quantified. For illustrative purposes, the telomere length measurements of Figure 1H were re-used here (indicated by transparent color). The mean is depicted in numbers and as black line, >150 measurements per group. (**C**) Quantification of gH2AX foci (>50 cells per group) in CD133− and CD133+ cells after 7 days vehicle or BIBR1532 treatment. Quantification and representative pictures of immunofluorescence staining of gH2AX foci are provided. (**D**) Senescent cells quantified by flow cytometry staining for SA-beta-Gal in CD133− (non-CSCs) and CD133+ (CSCs) after BIBR1532 or solvent treatment (7 days). (**E**,**F**) Apoptosis quantified by flow cytometry using double staining for CD133 and AnnexinV or (**E**) Caspase3/7 (**F**). In (**A**–**F**), data are represented as mean ± SEM. *n* = 3 independent experiments. * $p \leq 0.05$ (Mann–Whitney-U test), ns = not statistically significant.
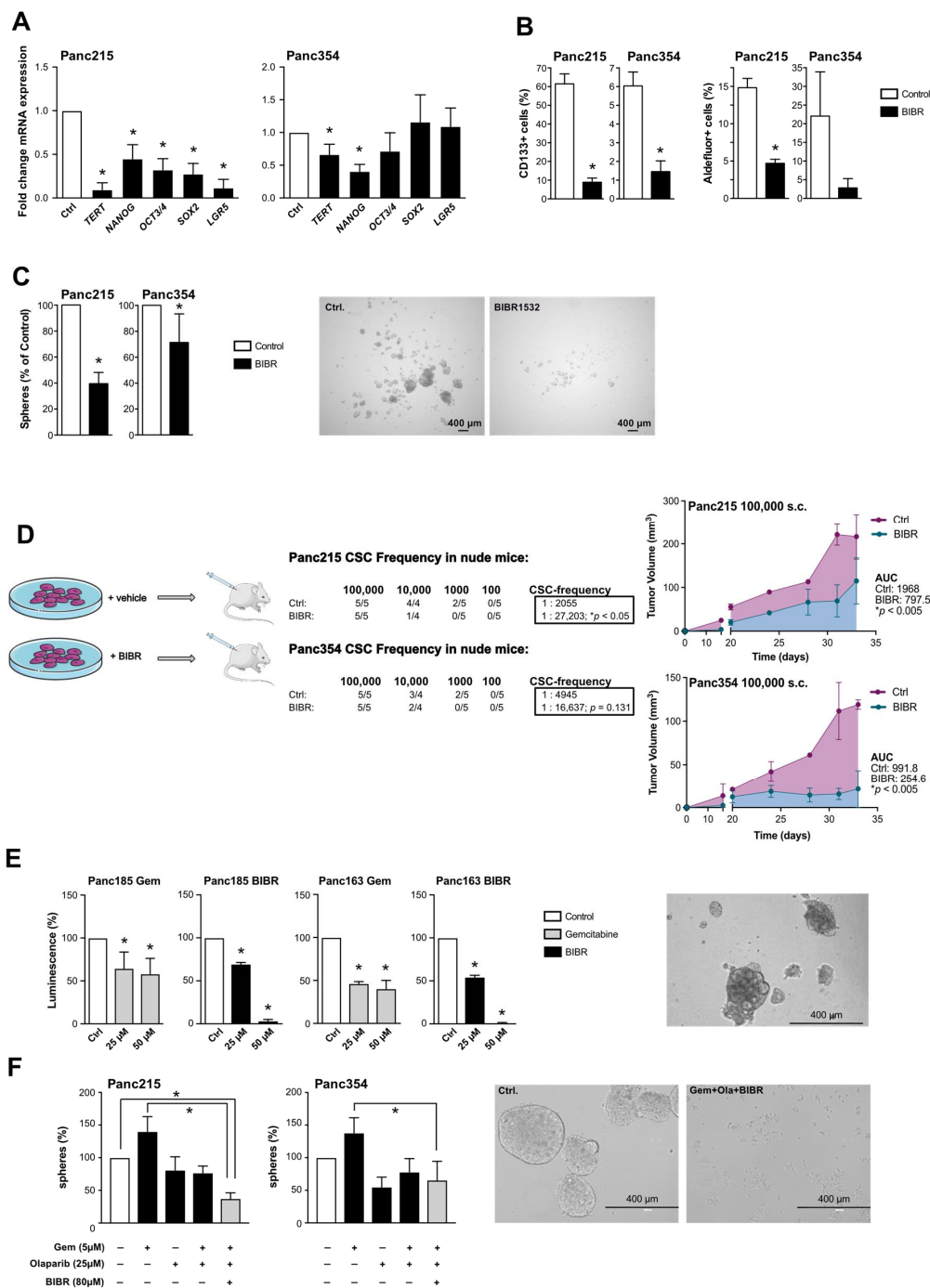
Figure 4. Telomerase inhibition as treatment strategy for pancreatic cancer (stem) cells: (**A**) Effects of the small molecule telomerase inhibitor BIBR1532 on the expression of TERT and pluripotency-associated genes as measured by RT-qPCR (*n* = 4 independent experiments). (**B**) Flow cytometry analyses for CD133 or ALDEFLUOR after BIBR1532 or solvent treatment (*n* = 3 independent experiments). (**C**) Quantification and representative pictures of spheres after BIBR1532 treatment (*n* = 3 independent experiments). (**D**) Schematic overview of BIBR1532 pre-treatment and in vivo experiment, number of tumorigenic cells within the whole population shown as cancer stem cell (CSC) frequencies as determined by extreme limiting dilution assays (ELDA) in nude mice, and tumor volume measured after injection of 100,000 BIBR1532 or solvent treated Panc215 and Panc354 cells (*n* ≥ 4 mice for each group). (**E**) Viability of PDX-derived organoids treated with gemcitabine and BIBR1532 at the indicated concentrations. (**F**) Quantification and representative pictures of sphere formation assays after single agent or combination treatment with gemcitabine, Olaparib, and BIBR1532 (*n* = 5 independent experiments). In (**A–C,E,F**) data are represented as mean ± SEM. * *p* ≤ 0.05 (Mann–Whitney-U test). In (**D**) data are represented as mean ± SEM. * *p* ≤ 0.05 (Area under the curve).

We have previously shown that chemotherapy enriches for CSCs, and have demonstrated the efficacy of combining stem cell inhibitors, stroma-depleting agents and chemotherapy to significantly improve survival of mice in vivo (among others: [15,23]). We next used organoid cultures to predict drug response in primary tumor cells as described previously [24]. In organoid cultures generated from primary pancreatic cancer cells we observed a significant decrease in luminescence (i.e., viability) upon treatment with increasing doses of gemcitabine. However, gemcitabine did not abrogate organoid formation, which was only achieved using BIBR1532 treatment (Figure 4E). As the induction of DNA damage by telomerase inhibition did not entirely abrogate CSC function (see Figure 3), we used a combination of chemotherapy, BIBR1532 and the PARP inhibitor Olaparib to target CSCs more successfully. Using sphere formation as a surrogate marker for CSC activity, combination therapy had significantly stronger effects than chemotherapy alone (Figure 4F).

3.5. Telomerase Inhibition as Novel Treatment Strategy for Pancreatic Cancer

In order to ensure that the effects of BIBR1532 are specific for telomerase inhibition, we proceeded to corroborate our main findings with shRNA-mediated TERT-knockdown (TERT-KD). As expected, genetic knockdown of TERT using two different shRNAs suppressed the expression of *TERT* (Figure 5A), and strongly suppressed telomerase activity (Figure 5B); due to its stronger effects, shRNA 340160 was used for all subsequent experiments. TERT-KD suppressed the expression of stemness-associated genes (Figure 5C). The reduction in stemness translated into depletion of CD133+ CSCs (Figure 5D) and reduced sphere formation activity (Figure 5E). Similar to the effects of BIBR1532 (Figure 3F,G), the TERT-KD significantly increased apoptosis in CD133+ cells but not in CD133− cells (Figure 5F). Most importantly, the TERT-KD strongly reduced TIC frequency in ELDA xenografting assays (Figure 5G, Supplementary Figure S7). These results closely resemble those achieved with BIBR1532, confirming that the effects observed above are indeed telomerase-specific.

To model the effects of telomerase inhibition as an applied treatment in vivo, we performed subcutaneous xenografting of Panc215 cells carrying an inducible shTERT cassette. Induction of the TERT-KD before injection with doxycycline resulted in significantly smaller tumors compared to scrambled control (Figure 5H). In a preclinical trial we xenografted inducible TERT-KD Panc215 cells and induced the knockdown 28 days after implantation, when tumors were firmly established. While dox-treated scrambled cells showed continuous tumor growth leading to sacrifice of the mice, we observed disease stabilization after TERT-KD (Figure 5I). The residual tumors showed downregulation of hTERT as well as decreased telomerase activity (Figure 5J). Histological analysis of the explanted tumors showed no gross differences between the two treatment groups with regard to tumor morphology, cellularity or stroma composition (Figure 5K). Altogether, these data indicate that TERT/telomerase inhibition depletes CSCs, resulting in disease stabilization in PDAC.
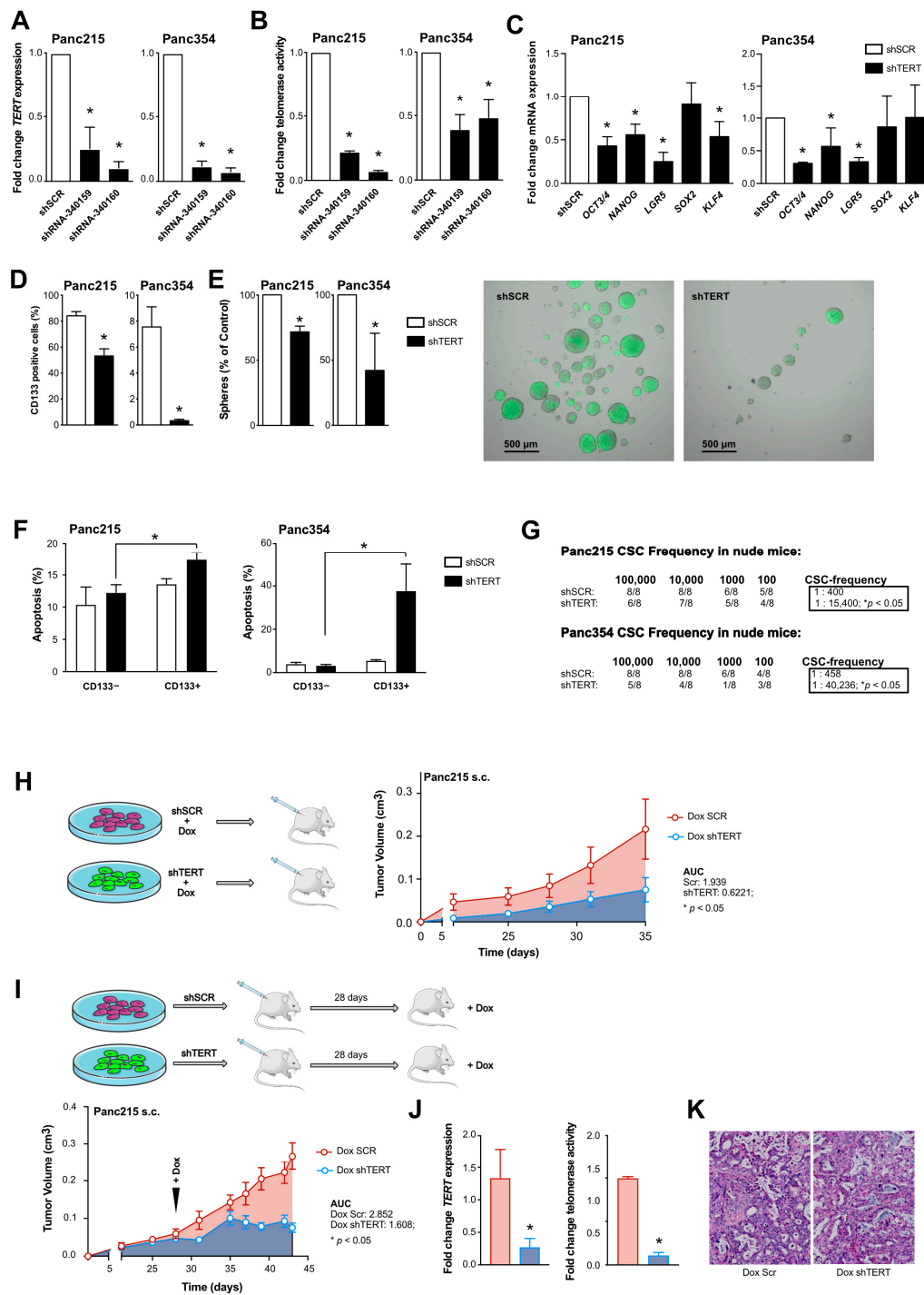
Figure 5. Knockdown of TERT diminishes pancreatic cancer stem cells: (**A**,**B**) Gene expression of TERT (**A**) and telomerase activity (**B**) in Panc215 and Panc354 cells transduced with shRNA-340159 and shRNA-340160 compared to scrambled (shSCR) control. (**C**) Expression levels of stemness/pluripotency-associated genes using shRNA-340160 (shTERT) for TERT mediated knockdown in Panc215 and Panc354 cells. (**D**,**E**) Flow cytometry analyses for CD133 (**D**) and sphere formation (**E**) upon TERT knock-down (KD) compared to scrambled (shSCR) control. (**F**) Quantification of apoptosis in shSCR and shTERT transduced cells (Panc215 and Panc354) using flow cytometry analysis for AnnexinV (*n* = at least 3 independent experiments). (**G**) In vivo tumor-initiating potential with CSC frequencies (number of tumorigenic cells within the whole population) as determined by ELDA in nude mice after TERT-KD compared to scrambled control (*n* = 8 animals); (**H**) Schematic illustration of in vivo experiment with cells carrying an inducible TERT-KD (Dox shTERT) or scrambled (Dox SCR) control construct. Cells were treated with doxycycline (DOX) 7 days before s.c. xenografting in nude mice. Graph shows time-dependent growth of subcutaneously engrafted tumors (*n* = 4 mice per group). (**I**) Schematic

illustration of in vivo experiment and visual representation of time-dependent tumor growth of subcutaneously (s.c.) engrafted tumors arising from TERT-KD and SCR cells, over the course of doxycycline treatment 28 days after s.c. xenografting in nude mice (*n* = 6 mice per group). Tumor growth is depicted until the first control mice had to be sacrificed. 4× magnification is shown (**J**) Gene expression of TERT and telomerase activity compared in TERT-KD and SCR tumors (induced with DOX at day 28) after sacrificing mice 43 days after xenografting. (**K**) representative H&E staining of at day 43 explanted TERT-KD and scrambled tumors (induced with DOX at day 28). In (**A–G,J**) data are represented as mean ± SEM. * $p \leq 0.05$ (Mann–Whitney-U test). In (**H,I**) data are represented as mean ± SEM. * $p \leq 0.05$ (Area under the curve).

4. Discussion

We and others have previously identified CSCs in pancreatic cancer, and have demonstrated that they play a key role in the propagation, chemoresistance and metastasis [5,6]. PDAC remains a disease that is terribly difficult to treat. Thus, eliminating CSCs as a continuous source of tumor growth, resistance and relapse is of utmost importance for improved clinical outcome. While functional differences in CSCs are continuously being discovered, the underlying mechanisms for their acquisition of stemness features are much less clear.

CSCs have been isolated based on different markers and cellular features. We have previously established CD133 expression and functional enrichment via sphere formation as reliable CSC markers in PDAC [5], and together with ALDEFLUOR activity these are most widely used. In addition to using these markers, we evaluated the expression levels of pluripotency-associated genes such as NANOG, OCT3/4, KLF4, SOX2 and others to overcome the limitations of the markers mentioned above, and additionally used a NANOG reporter system to further demonstrate stemness in the isolated CSCs.

Unlimited proliferation requiring telomere maintenance is a "hallmark of cancer" as indicated by Hanahan and Weinberg, and selective telomere maintenance or even elongation via telomerase activity is an essential feature of stem cells. However, available data on telomerase activity and its regulation in CSCs is scarce.

Increased telomere length has been reported in several tumor entities, such as prostate cancer and glioblastoma [25,26]. In contrast to these studies and our data, Joseph et al. surprisingly observed no such differences in breast and pancreatic cancer cells [27]. This might be explained by the use of only one established cell line versus the panel of primary cells used in our study, as well as by inter-tumoral heterogeneity. Interestingly, Joseph et al. did observe reduced tumor engraftment in nude mice under treatment with the telomerase inhibitor Imetelstat, indicating an effect on a CSC population. While a telomerase-independent mechanism of regulation was suggested by Joseph et al., and the use of high doses of BIBR1532 has also been shown to induce cytotoxicity irrespective of telomerase activity [28], our data clearly demonstrate the dependency of CSCs on intact telomere regulation. Specifically, we demonstrate that pharmacological inhibition or shRNA-mediated TERT-KD result in CSC depletion as evidenced by reduced expression of stemness genes and surface markers, and abrogation of sphere formation and tumorigenicity in vivo. While telomere length can be maintained by alternative lengthening of telomere (ALT) mechanisms in 10–15% of the tumors, the activation of ALT pathways is rare in cancer and most cancers maintain telomeres through regulation of telomerase activity [12]. Furthermore, the telomere staining pattern observed in our cells shows no indication for an important role of ALT.

Direct promoter activation may also lead to increased TERT activity in tumor cells, and two common promoter mutations (-124 and -146 bp upstream of the TERT start site) are typically associated with increased telomerase activity. While these mutations are frequent in other cancers, they rarely occur in GI-tumors [20], which is well in line with our own observation that all PDAC cells we tested showed wildtype promoter sequences.

Using BIBR1532 as a small molecule telomerase inhibitor, we detected a dose-dependent proliferation arrest, which is in line with reduced cell proliferation observed in ESCs. Critical shortening of telomeres induces DNA damage response pathways, cell-cycle arrest and finally cell death. These effects are triggered by ATM and/or ATR-dependent signaling

via checkpoint activation, resulting in the marking of uncapped chromosomal ends by formation of gH2AX foci and telomere dysfunction-induced foci (TIFs) [29]. Thus, the cellular response to dysfunctional telomeres is regulated through the same factors that control DNA damage response [30] and activate p53 and its downstream targets [31]. We have previously demonstrated that CD133+ CSCs exhibit enhanced DNA damage repair and are particularly sensitive to inhibition of ATR-mediated DNA damage response [32].

We observed that BIBR1532 treatment resulted in gH2AX foci formation and senescence in CD133+ cells. These effects were accompanied by preferential induction of apoptosis in the CSC population, emphasizing the dependency of CSCs on functional telomerase and stabilized telomeres. CSCs also appear to be more susceptible to telomerase inhibition-induced DNA damage and ultimately to the induction of apoptosis, which is especially interesting as other stem cells (ESCs and iPSCs) are particularly sensitive to DNA damage-induced apoptosis [33].

Because pancreatic CSCs are highly resistant to chemotherapy [6], their elimination is crucial to improve therapy efficacy and outcome for PDAC patients. We have repeatedly shown that the identification of stem cell features in CSCs, such as the activity of embryonic signaling pathways can result in novel treatment strategies to eliminate pancreatic CSCs, resulting in long-term survival of mice harboring PDAC [15,23]. Here we demonstrate a new approach to this goal and show that pancreatic CSCs are highly dependent on telomerase activity and telomere elongation, and that loss of telomerase activity by genetic knockdown or small molecule inhibitors eliminates patient-derived pancreatic CSCs. For this study we used a series of primary cell lines generated from patient-derived xenografts. While this inevitably leads to more heterogeneity when it comes to results, it is important to note that the underlying mechanisms as well as the effects of telomerase inhibition, both by small molecules and TERT-KD, are reproducible in all utilized cell lines, strongly supporting the significance of the results.

The prediction of drug response in vitro on 2D monolayer cultures is traditionally very difficult. 3D pancreatic organoid cultures better recapitulate the situation in a tumor and are superior to 2D cultures when it comes to drug testing [34]. Therefore, we generated organoid cultures from patient-derived xenografts for drug testing and detected a dose-dependent response of organoid viability to both BIBR1532 and gemcitabine treatment. To demonstrate the efficacy of a drug regimen against CSCs, however, tumor formation (or lack thereof) in vivo remains the gold standard. Therefore, we used an inducible TERT-KD construct, allowing for treatment to commence after tumor formation and growth, replicating the therapeutic scenario in a clinical setting without the confounding off-target effects of small molecule inhibitors. Indeed, we observed significantly smaller tumors whenever telomerase function was lost, indicating a crucial role for TERT in tumor propagation.

TERT-KD depletes CSCs, highlighting the dependency of CSCs on intact telomerase regulation. In this respect CSCs seem resemble human ESCs, where TERT has been shown to be an essential mediator of pluripotency, cell cycle progression and differentiation [35,36]. Furthermore, we observed that TERT-KD critically downregulates the core pluripotency factors OCT4, KLF4, SOX2, NANOG, and KLF4 is known to bind and activate the TERT promoter in human and mouse stem cells [37,38]. However, many of the transcription factors involved in the regulation of self-renewal and pluripotency in human ESCs are tightly intertwined; KLF4 binds and upregulates the NANOG promoter, which in turn is also regulated through cooperation of SOX2 and OCT4 with KLF4 [39,40]. Furthermore, silencing of OCT3/4 correlates with downregulation of pluripotency factors and TERT, with simultaneous activation of p53 and upregulation of its target genes p21 and PUMA [41]. The subsequent p53-dependent induction of cell cycle arrest, senescence, apoptosis and the suppression of pluripotency and self-renewal in ESCs as a result of DNA damage has also been demonstrated [42].

Thus, a tightly coordinated regulation of stemness-associated transcription factors and pathways is essential for the preservation of "stemness". We therefore hypothesized that TERT expression is regulated by the same transcription factor signature; Using a

NANOG reporter system we demonstrate that high NANOG expression correlates directly with TERT expression and vice versa, conferring increased CD133 expression and sphere formation ability to cancer cells. Using expression vectors for OCT3/4, SOX2, KLF4 and NANOG, we demonstrate that while all four pluripotency factors seem to increase TERT expression and thus impact the regulation of telomerase activity, SOX2 and OCT3/4 do so most strongly. In summary, these data show a previously undiscovered positive feed-back loop between pluripotency transcription factors and TERT regulation in pancreatic CSCs.

TERT is furthermore regulated by epigenetic changes, such as chromatin loop structures in cells with long telomeres [43] or through CpG islet methylation of the TERT promoter. However, epigenetic changes of TERT by methylation remain a controversial topic: Bechter et al. demonstrated that in patients with B-CLL, TERT promoter hypomethylation was associated with an increased telomerase activity [44], whereas others showed that TERT hypermethylation increases TERT mRNA expression and telomerase activity in a variety of cancers (e.g., bladder, brain, colon, heart and kidney) [45].

We found no differences in TERT promoter methylation using previously published global methylation data, suggesting that methylation is likely not a controlling factor in pancreatic CSCs.

5. Conclusions

In summary, our study demonstrates that telomerase regulation is critical for stemness maintenance in pancreatic CSCs and examines the effects of telomerase inhibition as a potential treatment option of pancreatic cancer. This significantly promotes our understanding of PDAC tumor biology and CSC regulation and may result in improved treatment for pancreatic cancer patients.

References

1. Rahib, L.; Smith, B.D.; Aizenberg, R.; Rosenzweig, A.B.; Fleshman, J.M.; Matrisian, L.M. Projecting cancer incidence and deaths to 2030: The unexpected burden of thyroid, liver, and pancreas cancers in the United States. *Cancer Res.* **2014**, *74*, 2913–2921. [CrossRef] [PubMed]
2. Siegel, R.L.; Miller, K.D.; Jemal, A. Cancer statistics, 2015. *CA Cancer J. Clin.* **2015**, *65*, 5–29. [CrossRef] [PubMed]
3. Von Hoff, D.D.; Ervin, T.; Arena, F.P.; Chiorean, E.G.; Infante, J.; Moore, M.; Seay, T.; Tjulandin, S.A.; Ma, W.W.; Saleh, M.N.; et al. Increased survival in pancreatic cancer with nab-paclitaxel plus gemcitabine. *N. Engl. J. Med.* **2013**, *369*, 1691–1703. [CrossRef] [PubMed]
4. Conroy, T.; Desseigne, F.; Ychou, M.; Bouche, O.; Guimbaud, R.; Becouarn, Y.; Adenis, A.; Raoul, J.L.; Gourgou-Bourgade, S.; de la Fouchardiere, C.; et al. FOLFIRINOX versus gemcitabine for metastatic pancreatic cancer. *N. Engl. J. Med.* **2011**, *364*, 1817–1825. [CrossRef]
5. Hermann, P.C.; Huber, S.L.; Herrler, T.; Aicher, A.; Ellwart, J.W.; Guba, M.; Bruns, C.J.; Heeschen, C. Distinct populations of cancer stem cells determine tumor growth and metastatic activity in human pancreatic cancer. *Cell Stem Cell* **2007**, *1*, 313–323. [CrossRef]
6. Li, C.; Heidt, D.G.; Dalerba, P.; Burant, C.F.; Zhang, L.; Adsay, V.; Wicha, M.; Clarke, M.F.; Simeone, D.M. Identification of pancreatic cancer stem cells. *Cancer Res.* **2007**, *67*, 1030–1037. [CrossRef]
7. Clarke, M.; Dick, J.; Dirks, P.; Eaves, C.; Jamieson, C.; Jones, D.; Visvader, J.; Weissman, I.; Wahl, G. Cancer Stem Cells—Perspectives on Current Status and Future Directions: AACR Workshop on Cancer Stem Cells. *Cancer Res.* **2006**, *66*, 9339–9344. [CrossRef]
8. Nakamura, T.M. Telomerase Catalytic Subunit Homologs from Fission Yeast and Human. *Science* **1997**, *277*, 955–959. [CrossRef]
9. DeLange, T. Shelterin: The protein complex that shapes and safeguards human telomeres. *Genes Dev.* **2005**, *19*, 2100–2110. [CrossRef]
10. Wright, W.E.; Piatyszek, M.A.; Rainey, W.E.; Byrd, W.; Shay, J.W. Telomerase activity in human germline and embryonic tissues and cells. *Dev. Genet.* **1996**, *18*, 173–179. [CrossRef]
11. Collado, M.; Blasco, M.A.; Serrano, M. Cellular senescence in cancer and aging. *Cell* **2007**, *130*, 223–233. [CrossRef] [PubMed]
12. Shay, J.W.; Wright, W.E. Telomeres and telomerase: Three decades of progress. *Nat. Rev. Genet.* **2019**, *20*, 299–309. [CrossRef]
13. Damm, K.; Hemmann, U.; Garin-Chesa, P.; Hauel, N.; Kauffmann, I.; Priepke, H.; Niestroj, C.; Daiber, C.; Enenkel, B.; Guilliard, B.; et al. A highly selective telomerase inhibitor limiting human cancer cell proliferation. *EMBO J.* **2001**, *20*, 6958–6968. [CrossRef]
14. Hu, Y.; Smyth, G.K. ELDA: Extreme limiting dilution analysis for comparing depleted and enriched populations in stem cell and other assays. *J. Immunol. Methods* **2009**, *347*, 70–78. [CrossRef]
15. Mueller, M.T.; Hermann, P.C.; Witthauer, J.; Rubio-Viqueira, B.; Leicht, S.F.; Huber, S.; Ellwart, J.W.; Mustafa, M.; Bartenstein, P.; D'Haese, J.G.; et al. Combined targeted treatment to eliminate tumorigenic cancer stem cells in human pancreatic cancer. *Gastroenterology* **2009**, *137*, 1102–1113. [CrossRef] [PubMed]
16. Lerma, L.; Alcala, S.; Piñero, C.; Torres, M.; Martin, B.; Lim, F.; Sainz, B.; Tabarés, E. Expression of the immediate early IE180 protein under the control of the hTERT and CEA tumor-specific promoters in recombinant pseudorabies viruses: Effects of IE180 protein on promoter activity and apoptosis induction. *Virology* **2016**, *488*, 9–19. [CrossRef] [PubMed]
17. Hotta, A.; Cheung, A.Y.; Farra, N.; Vijayaragavan, K.; Séguin, C.A.; Draper, J.S.; Pasceri, P.; Maksakova, I.A.; Mager, D.L.; Rossant, J.; et al. Isolation of human iPS cells using EOS lentiviral vectors to select for pluripotency. *Nat. Methods* **2009**, *6*, 370–376. [CrossRef] [PubMed]
18. Hummel, S.; Ferreira, M.S.V.; Heudobler, D.; Huber, E.; Fahrenkamp, D.; Gremse, F.; Schmid, K.; Muller-Newen, G.; Ziegler, P.; Jost, E.; et al. Telomere shortening in enterocytes of patients with uncontrolled acute intestinal graft-versus-host disease. *Blood* **2015**, *126*, 2518–2521. [CrossRef] [PubMed]
19. Takai, A.; Nakano, M.; Saito, K.; Haruno, R.; Watanabe, T.M.; Ohyanagi, T.; Jin, T.; Okada, Y.; Nagai, T. Expanded palette of Nano-lanterns for real-time multicolor luminescence imaging. *Proc. Natl. Acad. Sci. USA* **2015**, *112*, 4352–4356. [CrossRef]
20. Vinagre, J.; Almeida, A.; Populo, H.; Batista, R.; Lyra, J.; Pinto, V.; Coelho, R.; Celestino, R.; Prazeres, H.; Lima, L.; et al. Frequency of TERT promoter mutations in human cancers. *Nat. Commun.* **2013**, *4*, 2185. [CrossRef]
21. Hsieh, M.H.; Chen, Y.T.; Lee, Y.H.; Lu, J.; Chien, C.L.; Chen, H.F.; Ho, H.N.; Yu, C.J.; Wang, Z.Q.; Teng, S.C. PARP1 controls KLF4-mediated telomerase expression in stem cells and cancer cells. *Nucleic Acids Res.* **2017**, *45*, 10492–10503. [CrossRef] [PubMed]

22. Celeghin, A.; Giunco, S.; Freguja, R.; Zangrossi, M.; Nalio, S.; Dolcetti, R.; Rossi, A.D. Short-term inhibition of TERT induces telomere length-independent cell cycle arrest and apoptotic response in EBV-immortalized and transformed B cells. *Cell Death Dis.* **2016**, *7*, e2562. [CrossRef]

23. Lonardo, E.; Hermann, P.C.; Mueller, M.-T.; Huber, S.; Balic, A.; Miranda-Lorenzo, I.; Zagorac, S.; Alcala, S.; Rodriguez-Arabaolaza, I.; Ramirez, J.C.; et al. Nodal/Activin signaling drives self-renewal and tumorigenicity of pancreatic cancer stem cells and provides a target for combined drug therapy. *Cell Stem Cell* **2011**, *9*, 433–446. [CrossRef]

24. Frappart, P.O.; Walter, K.; Gout, J.; Beutel, A.K.; Morawe, M.; Arnold, F.; Breunig, M.; Barth, T.F.; Marienfeld, R.; Schulte, L.; et al. Pancreatic cancer-derived organoids—A disease modeling tool to predict drug response. *United Eur. Gastroenterol. J.* **2020**, *8*, 594–606. [CrossRef]

25. Beier, F.; Beier, C.P.; Aschenbrenner, I.; Hildebrandt, G.C.; Brummendorf, T.H.; Beier, D. Identification of CD133(-)/telomerase(low) progenitor cells in glioblastoma-derived cancer stem cell lines. *Cell Mol. Neurobiol.* **2011**, *31*, 337–343. [CrossRef]

26. Marian, C.O.; Wright, W.E.; Shay, J.W. The effects of telomerase inhibition on prostate tumor-initiating cells. *Int. J. Cancer* **2010**, *127*, 321–331. [CrossRef]

27. Joseph, I.; Tressler, R.; Bassett, E.; Harley, C.; Buseman, C.M.; Pattamatta, P.; Wright, W.E.; Shay, J.W.; Go, N.F. The telomerase inhibitor imetelstat depletes cancer stem cells in breast and pancreatic cancer cell lines. *Cancer Res.* **2010**, *70*, 9494–9504. [CrossRef] [PubMed]

28. El-Daly, H.; Kull, M.; Zimmermann, S.; Pantic, M.; Waller, C.F.; Martens, U.M. Selective cytotoxicity and telomere damage in leukemia cells using the telomerase inhibitor BIBR1532. *Blood* **2005**, *105*, 1742–1749. [CrossRef]

29. Sexton, A.N.; Regalado, S.G.; Lai, C.S.; Cost, G.J.; O'Neil, C.M.; Urnov, F.D.; Gregory, P.D.; Jaenisch, R.; Collins, K.; Hockemeyer, D. Genetic and molecular identification of three human TPP1 functions in telomerase action: Recruitment, activation, and homeostasis set point regulation. *Genes Dev.* **2014**, *28*, 1885–1899. [CrossRef]

30. Takai, H.; Smogorzewska, A.; de Lange, T. DNA Damage Foci at Dysfunctional Telomeres. *Curr. Biol.* **2003**, *13*, 1549–1556. [CrossRef]

31. Brassat, U.; Balabanov, S.; Bali, D.; Dierlamm, J.; Braig, M.; Hartmann, U.; Sirma, H.; Gunes, C.; Wege, H.; Fehse, B.; et al. Functional p53 is required for effective execution of telomerase inhibition in BCR-ABL-positive CML cells. *Exp. Hematol.* **2011**, *39*, 66–76. [CrossRef]

32. Gallmeier, E.; Hermann, P.C.; Mueller, M.T.; Machado, J.G.; Ziesch, A.; De Toni, E.N.; Palagyi, A.; Eisen, C.; Ellwart, J.W.; Rivera, J.; et al. Inhibition of ataxia telangiectasia- and Rad3-related function abrogates the in vitro and in vivo tumorigenicity of human colon cancer cells through depletion of the CD133(+) tumor-initiating cell fraction. *Stem Cells* **2011**, *29*, 418–429. [CrossRef]

33. Liu, C.C.; Ma, D.L.; Yan, T.D.; Fan, X.; Poon, Z.; Poon, L.F.; Goh, S.A.; Rozen, S.G.; Hwang, W.Y.; Tergaonkar, V.; et al. Distinct Responses of Stem Cells to Telomere Uncapping-A Potential Strategy to Improve the Safety of Cell Therapy. *Stem Cells* **2016**, *34*, 2471–2484. [CrossRef] [PubMed]

34. Griffith, L.G.; Swartz, M.A. Capturing complex 3D tissue physiology in vitro. *Nat. Rev. Mol. Cell. Biol.* **2006**, *7*, 211–224. [CrossRef] [PubMed]

35. Liu, L. Linking Telomere Regulation to Stem Cell Pluripotency. *Trends Genet.* **2017**, *33*, 16–33. [CrossRef]

36. Yang, C.; Przyborski, S.; Cooke, M.J.; Zhang, X.; Stewart, R.; Anyfantis, G.; Atkinson, S.P.; Saretzki, G.; Armstrong, L.; Lako, M. A key role for telomerase reverse transcriptase unit in modulating human embryonic stem cell proliferation, cell cycle dynamics, and in vitro differentiation. *Stem Cells* **2008**, *26*, 850–863. [CrossRef]

37. Hoffmeyer, K.; Raggioli, A.; Rudloff, S.; Anton, R.; Hierholzer, A.; Del Valle, I.; Hein, K.; Vogt, R.; Kemler, R. Wnt/beta-catenin signaling regulates telomerase in stem cells and cancer cells. *Science* **2012**, *336*, 1549–1554. [CrossRef]

38. Wong, C.W.; Hou, P.S.; Tseng, S.F.; Chien, C.L.; Wu, K.J.; Chen, H.F.; Ho, H.N.; Kyo, S.; Teng, S.C. Kruppel-like transcription factor 4 contributes to maintenance of telomerase activity in stem cells. *Stem Cells* **2010**, *28*, 1510–1517. [CrossRef]

39. Chan, K.K.; Zhang, J.; Chia, N.Y.; Chan, Y.S.; Sim, H.S.; Tan, K.S.; Oh, S.K.; Ng, H.H.; Choo, A.B. KLF4 and PBX1 directly regulate NANOG expression in human embryonic stem cells. *Stem Cells* **2009**, *27*, 2114–2125. [CrossRef]

40. Nakatake, Y.; Fukui, N.; Iwamatsu, Y.; Masui, S.; Takahashi, K.; Yagi, R.; Yagi, K.; Miyazaki, J.; Matoba, R.; Ko, M.S.; et al. Klf4 cooperates with Oct3/4 and Sox2 to activate the Lefty1 core promoter in embryonic stem cells. *Mol. Cell. Biol.* **2006**, *26*, 7772–7782. [CrossRef]

41. Zhang, H.H.; Li, S.Z.; Zhang, Z.Y.; Hu, X.M.; Hou, P.N.; Gao, L.; Du, R.L.; Zhang, X.D. Nemo-like kinase is critical for p53 stabilization and function in response to DNA damage. *Cell Death Differ.* **2014**, *21*, 1656–1663. [CrossRef]

42. Chin, L.; Artandi, S.E.; Shen, Q.; Tam, A.; Lee, S.L.; Gottlieb, G.J.; Greider, C.W.; DePinho, R.A. p53 deficiency rescues the adverse effects of telomere loss and cooperates with telomere dysfunction to accelerate carcinogenesis. *Cell* **1999**, *97*, 527–538. [CrossRef]

43. Kim, W.; Ludlow, A.T.; Min, J.; Robin, J.D.; Stadler, G.; Mender, I.; Lai, T.P.; Zhang, N.; Wright, W.E.; Shay, J.W. Regulation of the Human Telomerase Gene TERT by Telomere Position Effect-Over Long Distances (TPE-OLD): Implications for Aging and Cancer. *PLoS Biol.* **2016**, *14*, e2000016. [CrossRef]

44. Bechter, O.E.; Eisterer, W.; Dlaska, M.; Kuhr, T.; Thaler, J. CpG island methylation of the hTERT promoter is associated with lower telomerase activity in B-cell lymphocytic leukemia. *Exp. Hematol.* **2002**, *30*, 26–33. [CrossRef]

45. Guilleret, I.; Yan, P.; Grange, F.; Braunschweig, R.; Bosman, F.T.; Benhattar, J. Hypermethylation of the human telomerase catalytic subunit (hTERT) gene correlates with telomerase activity. *Int. J. Cancer* **2002**, *101*, 335–341. [CrossRef]